2009

# Cholesterol Exposure at the Membrane Surface Is Necessary and Sufficient to Trigger Perfringolysin O Binding

John J. Flanagan
Rodney K. Tweten
Arthur E. Johnson
Alejandro P. Heuck, *University of Massachusetts - Amherst*

Published in final edited form as:
*Biochemistry*. 2009 May 12; 48(18): 3977–3987. doi:10.1021/bi9002309.

# Cholesterol Exposure at the Membrane Surface Is Necessary and Sufficient to Trigger Perfringolysin O Binding†

**John J. Flanagan**[‡,¶], **Rodney K. Tweten**[||], **Arthur E. Johnson**[‡,⊥,#], and **Alejandro P. Heuck**[§,*]

[‡] Department of Biochemistry and Biophysics, Texas A&M University, College Station, Texas 77843

[||] Department of Microbiology and Immunology, University of Oklahoma Health Sciences Center, Oklahoma City, Oklahoma 73104

[⊥] Department of Chemistry, Texas A&M University, College Station, Texas 77843

[#] Department of Molecular and Cellular Medicine, Texas A&M Health Science Center, College Station, Texas 77843

[§] Department of Biochemistry and Molecular Biology, University of Massachusetts, Amherst, Massachusetts 01003

## Abstract

Perfringolysin O (PFO) is the prototype for the cholesterol-dependent cytolysins, a family of bacterial pore-forming toxins that act on eukaryotic membranes. The pore-forming mechanism of PFO exhibits an absolute requirement for membrane cholesterol, but the complex interplay between the structural arrangement of the PFO C-terminal domain and the distribution of cholesterol in the target membrane is poorly understood. Herein we show that PFO binding to the bilayer and the initiation of the sequence of events that culminate in the formation of a transmembrane pore depend on the availability of free cholesterol at the membrane surface, while changes in the acyl chain packing of the phospholipids and cholesterol in the membrane core, or the presence or absence of detergent-resistant domains do not correlate with PFO binding. Moreover, PFO association with the membrane was inhibited by the addition of sphingomyelin, a typical component of membrane rafts in cell membranes. Finally, addition of molecules that do not interact with PFO, but intercalate into the membrane and displace cholesterol from its association with phospholipids (e.g., epicholesterol), reduced the amount of cholesterol required to trigger PFO binding. Taken together, our studies reveal that PFO binding to membranes is triggered when the concentration of cholesterol exceeds the association capacity of the phospholipids, and this cholesterol excess is then free to associate with the toxin.

The cholesterol-dependent cytolysins (CDCs)[1] are a family of bacterial pore-forming toxins that act on cholesterol-containing eukaryotic membranes. There are more than 20 known

†This work was supported by National Institutes of Health Grants AI 37657 (to R.K.T. and A.E.J.), by the Robert A. Welch Foundation (Chair Grant BE-0017), and by start up funds from the University of Massachusetts (A.P.H.).

*Corresponding Author. 710 N. Pleasant St., Lederle GRT 816, Amherst, MA 01003. Phone: (413) 545-2497. Fax: (413) 545-3291. heuck@biochem.umass.edu.
¶Present address: Amicus Therapeutics, Inc., Cranbury, NJ.

SUPPORTING INFORMATION AVAILABLE

Detailed protocols for the expression, labeling, and purification of PFO derivatives, Förster resonance energy transfer (FRET) measurements, and steady-state fluorescence spectroscopy procedures. FRET analysis of the PFO binding to LUVs containing different amount of cholesterol. A figure describing the primary sequence for commonly used PFO derivatives. This material is available free of charge via the Internet at http://pubs.acs.org.

proteins of this toxin family that have been identified from different genera of Gram-positive bacteria such as *Streptococcus*, *Listeria*, *Clostridium*, *Bacillus*, and *Arcanobacterium* (1). This is a growing family of toxins as new members are being discovered (2–4). Since the CDCs share a high degree of primary sequence homology, it is believed that the toxins adopt similar three-dimensional structures and have similar cytolytic modes of action (5,6). Moreover, the recently reported crystal structures for the membrane attack complex/perforin showed that the structural and functional features of the CDCs are related to pore-forming proteins employed by eukaryotic immune systems (7,8).

CDCs are secreted as water-soluble monomers of 50–70 kDa that form large ring- and arc-shaped homo-oligomeric pores (~35–50 monomers per oligomer; approximately 250 Å in diameter) in cholesterol-containing membranes (9–13). Disruption of the host cell membrane by these pore-forming toxins is an important step in bacterial pathogenesis (1).

As do many other bacterial and viral proteins, the CDCs take advantage of a distinguishing feature of mammalian membranes, in this case the presence of cholesterol (14,15). Since cholesterol is essential for CDC cytolytic activity, and preincubation of the CDCs with cholesterol inhibited cytolysis, it was long thought that cholesterol functioned as a receptor for this family of toxins. However, recent findings have challenged this long-standing paradigm because not all CDCs require cholesterol to bind to the membrane. For example, intermedilysin recognizes and binds the human CD59 protein (16). However, cholesterol is still required for the cytolytic activity of intermedilysin (17).

Perfringolysin O (PFO) is a prototype of the CDC family (6,18). Cytolysis starts when the C-terminal domain 4 of PFO (residues 391–500) first contacts the target membrane (19). Domain 4 has a beta-sandwich structure that interacts with the membrane surface only at one end via the loops that connect the two beta sheets in the domain (20–22). One of these loops, an 11 amino acid-residue sequence known as the Trp-rich loop, is highly conserved among most of the CDCs (1). Modifications in this conserved undecapeptide typically inhibit the hemolytic activity of the toxin by blocking the conformational changes that are required to allosterically trigger the insertion of the transmembrane beta-barrel (5,23,24). The correlation between this highly conserved amino acid sequence and the absolute cholesterol dependence led researchers to hypothesize that this undecapeptide represented the cholesterol binding site for the CDCs (25). However, it has recently been shown that cholesterol recognition and toxin binding are mediated by the other three loops, while the insertion of the undecapeptide may be coupled to the insertion of the transmembrane beta-barrel (24). Despite these important observations, the exact mechanism by which PFO interacts with cholesterol remains unclear.

We have recently shown that the binding of PFO solely to cholesterol is sufficient to trigger the conformational changes that effect oligomerization and initiate pore formation (26). However, substantial cholesterol (>30 mol%) is required to trigger the PFO membrane-interaction in bilayers comprised of cholesterol and phospholipids (19,27). It was therefore suggested that PFO binds to cholesterol rich-domains or membrane "rafts" (28). Yet, recent studies showed no correlation between the sterol structures that promote formation of liquid ordered ($l_o$) phases in liposomal membranes (or membrane "rafts" in cell membranes) and their ability to promote PFO-membrane interactions (29). In contrast, PFO binding to membranes was enhanced when the interaction between the sterol and the phospholipid acyl chains was weak (29,30). Taken together, these studies support the concept that there is a complex interplay

[1]PFO, perfringolysin O; CDCs, cholesterol-dependent cytolysins; $l_o$, liquid ordered; SM, sphingomyelin; $PFO^{C459A}$ is an example of the notation for the PFO derivative where the Cys459 was mutated to Ala; IANBD, *N,N'*-dimethyl-*N*-(iodoacetyl)-*N'*-(7-nitrobenz-2-oxa-1,3-diazol-4-yl)ethylene diamine; DPH, 1,6-diphenyl-1,3,5-hexatriene; PC, phosphatidylcholine; SDS, sodium dodecyl sulfate; AGE, agarose gel electrophoresis; TX-100, Triton X-100; LUVs, large unilamellar vesicles; TMH, transmembrane beta-hairpin; $l_d$, liquid disordered.

between the structural arrangement of the domain 4 loops and the distribution of cholesterol in the target membrane (27).

To better understand the nature of this complex PFO-cholesterol interaction in the context of membrane phospholipids, we have systematically examined the phospholipid dependence of PFO binding. Our studies reveal that (i) the interactions between phospholipids and cholesterol in the bilayer dictate the cholesterol threshold for PFO binding; (ii) PFO binding to the target membrane is not detectably dependent on the packing of the lipids in the membrane core; (iii) PFO binding does not correlate with the presence of a detergent-resistant fraction in the membrane; (iv) PFO association with the membrane was inhibited by the increase in the sphingomyelin (SM) content that is important for the establishment of membrane "rafts" in cell membranes; and (v) the cholesterol threshold required for PFO binding was reduced by the addition of sterols that do not interact with PFO, but do intercalate between the cholesterol molecules and interact with phospholipids. Taken together, our studies reveal that PFO membrane-binding is triggered when the concentration of cholesterol exceeds the association capacity of the phospholipids. Packing of lipid molecules in the bilayer will dictate whether or not cholesterol is accessible to PFO. The excess of cholesterol is then free to associate with the toxin and trigger the conformational changes required for toxin oligomerization and pore formation.

## EXPERIMENTAL PROCEDURES

### Cloning and Mutagenesis of the PFO Gene

The gene encoding $PFO^{C459A}$, derived from PCR amplification of PFO from pRT20 (31), was cloned into the *Bgl*II and *Eco*RI sites of the expression vector pRSETB (Invitrogen) in order to remove an extra Trp residue that was introduced into the protein by the original expression vector (pAH21, see Supporting Information). The expressed PFO derivative contained a polyhistidine tag and enterokinase cleavage site at its N-terminus. When the polyhistidine tag is removed, the expressed protein consists of the mature PFO (beginning with amino acid K29) fused to six amino acids (DPSSRS) carried over from the expression vector at its N-terminus. Since no significant functional or structural differences were found between PFO derivatives containing or lacking the polyhistidine tag, the pAH21 derivative of PFO was used (data not shown).

### Expression, Purification, and Labeling of PFO Derivatives

The expression, purification, and labeling with *N*, *N*′-dimethyl-*N*-(iodoacetyl)-*N*′-(7-nitrobenz-2-oxa-1,3-diazol-4-yl)ethylene diamine (IANBD, Invitrogen) of recombinant PFO derivatives were done with some modifications of previous procedures (31), as detailed in the Supporting Information.

### Liposome Preparation

1-Palmitoyl-2-oleoyl-*sn*-glycero-3-phosphocholine (POPC), 1,2-dioleoyl-*sn*-glycero-3-phosphocholine (DOPC), 1-stearoyl-2-oleoyl-*sn*-glycero-3-phosphocholine (SOPC), 1,2-dimyristoyl-*sn*-glycero-3-phosphocholine (DMPC), 1,2-dipalmitoyl-*sn*-glycero-3-phosphocholine (DPPC), 1,2-distearoyl-*sn*-glycero-3-phosphocholine (DSPC), bovine brain sphingomyelin (SM), and 1,2-dioleoyl-*sn*-glycero-3-phosphoethanolamine-*N*-(5-dimethylamino-1-napthalenesulfonyl (dansyl-PE) were obtained from Avanti Polar Lipids. Cholesterol (5-cholesten-3 -ol) and 3-epicholesterol (5-cholesten-3α-ol) were obtained from Steraloids. To quantify the percent recovery of both phospholipid and cholesterol during liposome preparations, trace amounts of [$^{14}$C]phospholipid and [$^{3}$H]cholesterol were added to each batch of liposomes. For POPC-, DOPC-, and SOPC- cholesterol liposomes, L-3-phosphatidylcholine-1,2-di[$^{14}$C]oleoyl (114 mCi/mmol; GE Healthcare) and [1,2-$^{3}$H(N)]

cholesterol (48.3 Ci/mmol; NEN, Boston, MA) were added. For DMPC-cholesterol, DPPC-cholesterol, and DSPC-cholesterol liposomes, L-3-phosphatidylcholine-1-palmitoyl-2[1-$^{14}$C] palmitoyl (110mCi/mmol; PerkinElmer) and [1,2-$^{3}$H(N)]cholesterol were added. Mixtures of phospholipid and cholesterol were dried under a stream of nitrogen at a temperature approximately 10 °C above the $T_m$ of the phospholipid. The dried lipid mixture was then dried further under a vacuum for 3 h. The dried phospholipid/cholesterol mixture was resuspended in 0.55 mL of buffer A [50 mM HEPES (*N*-2-hydroxyethly piperazine-*N*-2-ethanesulfonic acid) (pH 7.5), 100 mM NaCl] and vortexed until the dried lipid was fully hydrated (100 micromolar total lipid). LUVs comprised of POPC-sterol or DOPC-sterol were generated using an Avestin Liposofast extruder as described previously (31,32). For preparation of DMPC-sterol, DPPC-sterol, DSPC-sterol, and DOPC-SM-sterol liposomes, an Avanti mini extruder and heat block were used to ensure the liposomes were maintained at least 10 °C above the $T_m$ of the major phospholipid during generation of the vesicles. The percentage recovery of phospholipid and cholesterol ranged from 88 to 100% for all liposomes prepared. For 1,6-diphenyl-1,3,5-hexatriene (DPH) incorporation into liposomes, 1 L of a 280 M DPH (dissolved in dimethylformamide) solution was added to 550 L of liposomes in buffer A. These conditions created a molar ratio of DPH/lipid of 1:200 while also keeping the amount of organic solvent added to the liposomes at a minimum (≪1% of final volume). The liposome–DPH mixture was incubated for 1 h at 20–23 °C in the dark to prevent any photodegradation of the fluorescent probe.

## Steady-State Fluorescence Spectroscopy

Fluorescence equipment and measurements procedures were done as detailed previously with some modifications described in Supporting Information. For Trp intensity measurements, the excitation and emission wavelengths were 295 and 348 nm, respectively, with a 4 nm band-pass. For DPH anisotropy measurements, the excitation and emission wavelengths were 350 and 452 nm, respectively, with a 4 nm band-pass.

## Trp Fluorescence

For the spectroscopic analysis of PFO-membrane interactions, 250 L aliquots of 50 nM purified PFO$^{C459A}$ in buffer A were distributed into phosphatidylcholine (PC)-coated quartz microcuvettes. After the initial net (after blank subtraction) fluorescence intensity ($F_0$) of each sample was measured, each cuvette received 13.5 L of 1 mM liposomes (total lipid). The PFO-liposome samples were mixed and incubated at 37 °C for 30 min. After re-equilibration back to 25 °C, the net (after blank subtraction and dilution correction) emission intensity (F) of each sample was measured. The change in the Trp emission intensity was expressed as $F/F_0$.

## Anisotropy

The steady-state anisotropy of DPH in liposomes was measured in the L-format using Glan-Thompson prism polarizers in both the excitation and emission beams. The emission intensity measured when a 250- L sample was excited by vertically polarized light and the signal was detected through a horizontal polarizer was designated as $I_{VH}$. $I_{HH}$, $I_{HV}$, and $I_{VV}$ were defined analogously. The component intensities of a DPH-free liposome sample were subtracted from the corresponding component intensities of a DPH-containing liposome sample to obtain the net DPH emission intensities of a given sample. The fluorescence anisotropy was then calculated from

$$r=[\mathrm{net}I_{VV} - G(\mathrm{net}I_{HV})]/[\mathrm{net}I_{VV} + 2G(\mathrm{net}I_{VH})]$$

where the grating factor $G = \text{net}I_{VH}/\text{net}I_{HH}$.

### SDS–AGE Analysis of PFO Oligomers

Denaturing sodium dodecyl sulfate agarose gel electrophoresis (SDS–AGE) was carried out as previously described (33). Briefly, a 20 L sample containing 0.5 M NBD-labeled PFO and 0.5 mM liposomes (total lipid) was incubated for 30 min at 37 °C. After the incubation, one-third volume of sample buffer [0.1% (w/v) bromophenol blue, 45% (v/v) glycerol, 6% (w/v) SDS, 150 mM Tris-HCl (pH 6.8), 300 mM -mercaptoethanol] was added. The reaction mixture was then loaded onto a 1.5% (w/v in buffer A) agarose gel (10 cm × 6 cm × 0.5 cm) and run at 100 V for 40 min. After electrophoresis, the gel was scanned using a BioRad Molecular Imager FX with the external laser set to 488 nm to excite the NBD-labeled PFO.

### Triton X-100 Solubility

For detergent-insolubility assays, 30 L of 5 mM liposomes (total lipid) was added to 170 L of chilled 0.6% (v/v) TX-100 in buffer A. The detergent-liposome reactions were incubated on ice for 30 min, and then the entire reaction (200 L) was centrifuged in a TLA 100.2 rotor (Beckman) at 217000*g* for 1 h at 4 °C. The supernatant was carefully removed and the amount of [$^{14}$C] phosphatidylcholine and/or [$^{3}$H] cholesterol in both the supernatant and the pellet (if any) was determined after detergent extraction and ultracentrifugation.

## RESULTS

### Phospholipid Dependence of Cholesterol Requirement for PFO binding to Liposomes

It was shown previously that the interaction of PFO with cholesterol-containing liposomes requires a considerable amount of cholesterol to be present in target bilayers (19,34). We found this observation striking since PFO can form holes in mammalian endoplasmic reticulum membranes where the cholesterol content is known to be quite low (35–39). These apparently conflicting observations led us to examine more closely the relationship between PFO's cytolytic mechanism and the cholesterol content in model membrane systems.

Fluorescence spectroscopy was used to quantify the cholesterol dependence of PFO binding to large unilamellar vesicles (LUVs) composed of a simple binary mixture of cholesterol and PC. These LUVs consisted of increasing amounts of cholesterol with different PC species that varied both in the length and degree of saturation of their acyl chains (Table 1). The extent of PFO binding to different liposome preparations was monitored by the increase in PFO Trp emission intensity when Trp residues in domain 4 were exposed to the hydrophobic core of the membrane bilayer (19,21).

PFO showed a remarkable range of ability to bind membranes composed of different PC species. PFO bound to liposomes containing diunsaturated DOPC at ~5 mol% lower cholesterol concentrations than to liposomes containing monounsaturated SOPC (Figure 1A) or saturated DSPC (Figure 1B). Thus, the extent of PC acyl chain unsaturation is an important variable in determining the cholesterol content required for PFO binding.

The phospholipid acyl chain length also affects PFO binding, though less dramatically than acyl chain unsaturation. Increasing the length of the saturated acyl chain at the sn-1 position by two carbons (SOPC, 18 carbons vs POPC, 16 carbons; Table 1) lowered the cholesterol content required for PFO binding for mono-unsaturated PCs (Figure 1A), albeit only modestly. To further examine how the phospholipid acyl chain length influences PFO's ability to recognize cholesterol in membranes, binding was measured using cholesterol-containing liposomes and PCs with completely saturated acyl chains that were 14, 16, or 18 carbons in length (Table 1). As in the above experiments, the change in Trp emission intensity was used

to monitor PFO binding to the LUVs containing saturated PCs and cholesterol. In contrast to PFO binding to liposomes having at least one unsaturated acyl chain, a greater concentration of cholesterol was required for PFO to interact with saturated PC/cholesterol liposomes (Figure 1B). Only minimal PFO binding to DMPC/cholesterol liposomes is observed, unless the cholesterol concentration is higher than 50 mol%. But as the acyl chains were lengthened by two or four carbons (DPPC or DSPC, respectively), the amount of cholesterol needed for PFO binding was lowered, and the cholesterol dependence profiles were shifted toward the one for POPC/cholesterol.

## Cholesterol Requirement for PFO Oligomerization on PC-Liposomes

The above fluorescence experiments examined the binding of PFO to cholesterol-containing membranes. However, the experiments did not address whether the subsequent steps of the PFO cytolytic mechanism, oligomerization, and transmembrane beta-hairpin (TMH) insertion (19,32,33,40) had the same cholesterol dependence. Since oligomerization and TMH insertion occur after PFO binds to the membrane, it is conceivable that the cholesterol requirement would not be the same for these steps.

To test whether or not oligomerization occurred on the different PC-liposomes, we employed a technique known as SDS–AGE to monitor PFO oligomerization because PFO oligomers exhibit significant or complete resistance to dissociation by SDS. This technique has already been used to show that PFO forms large, oligomeric prepore complexes prior to insertion of its membrane-spanning TMHs (33). Therefore, the extent (if any) of PFO oligomerization on the various cholesterol-containing membranes can be determined by the presence of an SDS-resistant oligomeric band.

The degree of PFO oligomerization was determined by incubating cholesterol-containing liposomes with NBD-labeled $PFO^{D397C, C459A}$ (a PFO derivative labeled with a fluorescent NBD dye at position 397, hereafter termed NBD-PFO) and resolving the PFO samples on a 1.5% agarose gel. The Asp397 residue is water-exposed in the PFO monomer, and after oligomerization remains exposed to the aqueous solvent. Substitution of Asp397 for Cys and labeling with NBD did not modify the pore-forming properties of the toxin (21). For these experiments, we focused on POPC- and DOPC-cholesterol liposomes since these liposome compositions showed a large disparity in their cholesterol dependence curves of PFO binding (Figure 1A). NBD-PFO oligomerization on POPC- and DOPC-cholesterol liposomes (Figure 2, lanes A–F and G–L, respectively) showed the same dependence on cholesterol concentration as Trp-detected PFO binding to liposomes (Figure 1A).

In addition to examining the cholesterol concentration dependence of PFO binding to and oligomerization on various PC liposomes, we observed that the same cholesterol dependence held true for both TMH insertion (19) and pore formation (data not shown). Therefore, the above results, taken in total, indicate that the length and degree of saturation of the phospholipid acyl chains comprising the bilayer, along with the amount of cholesterol, dictate when cytolysis occurs. If PFO cannot bind to the membrane, then the subsequent steps (oligomerization, TMH insertion, and pore formation) in the cytolytic mechanism will not occur. Since the primary effect of changing phospholipids is to alter the amount of cholesterol required, it suggests that the ability of PFO to recognize and/or interact with cholesterol at the membrane surface is influenced by changing the physicochemical and/or steric properties of the phospholipid acyl chains and membranes.

## The Relative Ordering of the Phospholipid Acyl Chains does not Influence PFO Binding to Membranes

One of the major concerns when changing the phospholipid and sterol compositions of a membrane is the effect the change may have on the dynamics of the lipid bilayer. Generally, membrane fluidity reflects the motion and order (i.e., packing) of the various lipids within a membrane bilayer. To assess membrane fluidity, small fluorescent probes are often incorporated into bilayers to measure the acyl chain packing of the phospholipids. A large body of work on model membrane systems demonstrates that the molecular order and dynamics of the lipid chains are drastically affected by the introduction of double bonds into the fatty acid chains of the lipid. In addition, the presence of cholesterol in the membrane has an impact on the physical state and order of the surrounding lipids (refs 41 and 42 and references cited therein).

To measure the relative acyl chain packing of the various PC/cholesterol liposomes used in this study, we incorporated the fluorescent probe DPH into our cholesterol-containing liposomes and measured the steady-state anisotropy of the probe. Figure 3 summarizes these results for DPH incorporated at 0.5 mol% into the liposomes. For DPPC- and DSPC-cholesterol liposomes at 25 °C, the steady-state anisotropy is high (0.33–0.34) and nearly constant from 30 to 52 mol% cholesterol. These results are consistent with a high degree of acyl chain order that is independent of the high amount of cholesterol present in the membrane.

We also compared the steady-state anisotropy of DPH in monounsaturated POPC and diunsaturated DOPC as a function of cholesterol concentration. For these cholesterol-containing membranes at 25 °C, DPH steady-state anisotropies were lower throughout the entire cholesterol range when compared to the disaturated PCs, consistent with more freedom of motion of the DPH probe in the unsaturated acyl chain environment of POPC or DOPC. Increasing the cholesterol concentration results in an approximately linear increase in DPH anisotropy, indicating that cholesterol restricts the molecular motion of the acyl chains, though to a lesser extent than in the presence of disaturated phospholipids.

When comparing anisotropy values obtained at the same cholesterol concentration for the various phospholipids/cholesterol mixtures, the difference in DPH anisotropy values can be attributed to the presence of the double bonds in the unsaturated acyl chains that tend not to pack together as tightly as the saturated acyl chains. These results clearly show that the relative acyl chain packing in the hydrophobic core of the membrane is sensitive both to the phospholipid/cholesterol ratio and to the degree of unsaturation of the phospholipid acyl chains. However, it is also clear that when comparing the liposome compositions that support PFO binding (Figure 1A,B) to the DPH anisotropy values of those liposomes (Figure 3), there is no correlation between the DPH-detected lipid packing and the ability of PFO to recognize the cholesterol molecules in the liposomes.

The above DPH anisotropies were measured at 25 °C, yet PFO was incubated with liposomes at 37 °C in the above Trp binding experiments. Since changes in temperature may affect the properties of a membrane, we also measured the DPH anisotropy of the liposomes at 37 °C and found no significant change in the anisotropy profiles obtained at these temperatures (data not shown) (43). Therefore, we conclude that the packing of the phospholipids acyl chains and cholesterol into the membrane core does not dictate whether or not PFO binds to the bilayer surface.

## PFO Binds to Membranes Containing High Cholesterol Content Independently of Their Detergent Solubilization Properties

The above DPH anisotropy experiments provided some information regarding the overall behavior of the lipids in the liposomes (i.e., degree of lipid order). To determine if PFO binding to membranes correlated with the presence of detergent-resistant membranes in PC/cholesterol liposomes, we determined the extent of detergent-insoluble lipid material in various liposomes and compared the results to the PFO binding data. The PC/cholesterol liposomes were made with trace amounts of [$^3$H] cholesterol and [$^{14}$C] phosphatidylcholine so that we could determine the amount of insoluble membrane material by performing solubilization experiments with cold TX-100. The PC/cholesterol liposomes were then subjected to extraction with 0.6% (v/v) TX-100 at 0 °C, followed by ultracentrifugation to pellet any insoluble lipid material (44). The data revealed that the percentage of insoluble PC and cholesterol (amount of pelleted material) varied depending on the degree of saturation of the PC. At concentrations of ~30 mol% and above the saturated PC lipids, DPPC (Figure 4) or DMPC (data not shown) had the highest percentage of cholesterol and PC (92–100%) in the pellet regardless of the amount of cholesterol in the liposomes. The large amount of insoluble lipid in DPPC- and DMPC-cholesterol liposomes correlates with the lipids being in the $l_o$ phase, as suggested by their respective lipid/cholesterol phase diagrams (45,46). These $l_o$ phases have been shown to be more resistant to solubilization by detergents than $l_d$ ones (47).

In contrast to the saturated PC/cholesterol liposomes, DOPC/cholesterol liposomes were completely solubilized in cold TX-100, as shown by the lack of insoluble PC or cholesterol (Figure 4). The poor interaction between DOPC and cholesterol prevented the packing of the acyl chains, making the lipids more susceptible to detergent solubilization. Interestingly, the detergent insolubility data with POPC/cholesterol liposomes revealed insolubility properties that were intermediate between those of the saturated- and diunsaturated-cholesterol liposomes. In POPC liposomes, the percentage of insoluble cholesterol and PC in the pellet increased with increasing cholesterol concentrations (Figure 4). Since POPC contains both a saturated acyl chain and an unsaturated acyl chain, membranes containing POPC can form the $l_o$ phase when mixed with sufficient amounts of cholesterol (44,48). Therefore, increasing the cholesterol concentration in POPC liposomes appears to contribute to the packing of the acyl chains making the lipids more resistant to detergent solubilization. Since the ratio of [$^{14}$C] phospholipid/[$^3$H]cholesterol in the pellet was constant, cold TX-100 did not preferentially solubilize either cholesterol or phospholipid from the liposomes.

If PFO binding to membranes was based solely on whether the membranes are either detergent-resistant, detergent-soluble, or a combination of both properties, then there should be a correlation between the presence of these solubilization properties and PFO binding. However, PFO was able to bind to membranes being detergent-resistant (DMPC, DPPC, POPC) or detergent-soluble (DOPC), albeit at different cholesterol concentrations. For example, DOPC/cholesterol liposomes are detergent-soluble at either 30- or 50-mol% cholesterol (Figure 4), yet PFO binds only to the liposomes containing 50 mol% cholesterol (Figure 1A). Similarly, DPPC/cholesterol liposomes are mostly detergent-insoluble at all cholesterol concentrations (Figure 4), yet PFO binds only to the liposomes containing at least 50 mol% cholesterol (Figure 1B). Thus, the detergent solubility properties of membranes do not appear to be associated with PFO recognition of and binding to cholesterol-containing membranes.

## Sphingolipid–Cholesterol Interaction Reduces the Ability of PFO to Recognize Cholesterol on the Membrane Surface

All of the above experiments were performed on liposomes composed of a binary mixture of lipids (i.e., cholesterol and PC), yet biological membranes contain a variety of lipid species possessing different lengths of acyl chains, head groups, and number of double bonds. Since

one of the objectives of this work is to elucidate the role of phospholipids in PFO binding to cholesterol-containing membranes, we decided to examine PFO binding to liposomes composed of a more complex lipid mixture. In doing so, we prepared a series of liposomes containing a mixture of DOPC, cholesterol, and SM to see if the presence of sphingolipids influenced PFO binding and oligomerization. Since liposomes containing 60 mol% DOPC and 40 mol% cholesterol supported PFO binding (Figure 1A), liposomes were prepared with at least 40 mol% cholesterol and varying proportions of DOPC and SM in the nonsterol lipid.

As the amount of SM was increased in the nonsterol fraction from 17% to 50% SM, the change in PFO Trp emission intensity decreased, thereby suggesting that PFO does not recognize or bind cholesterol in membranes that contain a high percentage of sphingolipids (Figure 5A). However, since the presence of SM in the membrane modifies the spectral properties of the membrane-bound Trp residues (data not shown), a direct correlation between PFO binding and the total SM content cannot be ascertained from this data. The extent of PFO binding as the concentration of SM increase in the membrane was also determined by measuring formation of oligomers by NBD-PFO on DOPC/SM/cholesterol. Oligomerization is a good reporter for the cholesterol-dependent PFO–membrane interaction because PFO does not oligomerize in solution (49) or in the absence of cholesterol (26). The amount of PFO oligomerization decreased as the percentage of SM in the nonsterol fraction increased (Figure 5B). Thus, replacing DOPC molecules in the bilayer with SM caused a reduction in PFO binding to and oligomerization on the membrane.

Although the mol% of membrane cholesterol remained constant, replacing the unsaturated DOPC with the saturated sphingolipid species clearly affected PFO's ability to recognize and bind to cholesterol in the membranes. Since it has been shown previously that sphingolipids preferentially interact with sterols in both biological and model membranes and form detergent-resistant membranes (50), we measured the amount of insoluble material present in the DOPC/SM/cholesterol membranes by performing TX-100 insolubility assays. The DOPC/SM/cholesterol membranes contained a trace amount of [$^3$H]cholesterol in order to determine the amount of cholesterol present in the detergent-resistant fraction. After incubation with cold nonionic TX-100, the samples were pelleted, and the amount of radioactive cholesterol recovered in the pellet was plotted as a function of the initial percentage of SM in the nonsterol fraction. When the membranes contained no or very little SM, most of the [$^3$H]cholesterol was found in the supernatant and no lipid pellet was observed after incubation with TX-100 (Figure 5C). However, as the amount of SM increased in the cholesterol-containing membranes, a detergent-resistant pellet started to appear, and the percentage of [$^3$H]cholesterol found in the pellet increased (Figure 5C). When the nonsterol fraction of the membranes contained an equimolar amount of DOPC and SM (30 mol% apiece), approximately 40% of the [$^3$H]cholesterol could be found in the detergent-resistant pellet. The amount of [$^3$H]cholesterol found in the detergent-resistant pellet increased to roughly 80% when the nonsterol fraction was entirely SM. Since the formation of a detergent-resistant sphingolipid-cholesterol phase coincided with a decrease in PFO binding to the DOPC/SM/cholesterol membranes, it appears that PFO does not recognize or bind to cholesterol that is sequestered into sphingolipid-cholesterol rich domains.

## Only a Limited Number of the Cholesterol Molecules in the Membrane Are Accessible to Interact with PFO

Early experiments demonstrated that some sterols that are structurally related to cholesterol had an inhibitory effect on the hemolytic properties of the CDC bacterial toxins (51,52). From those inhibition studies, the structural and stereospecific requirements for the sterol molecule were identified. One such requirement was the presence of a hydroxyl group in the - configuration on carbon-3 of ring A of the cyclopentanoperhydrophenanthrene ring of

cholesterol. However, if the hydroxyl group was in the α-configuration, as in epicholesterol, then the sterol did not inhibit toxin activity because the toxin presumably could not recognize the sterol derivative (26,53).

To examine how cholesterol packing in the bilayer affects PFO interactions with the membrane, we took advantage of the inability of PFO to recognize epicholesterol and performed competition experiments with these two sterols. Since the stereochemistry of the polar –OH group is the only difference between cholesterol and epicholesterol, it has been suggested that the flat four-ring portions of the two sterols pack similarly with phospholipid acyl chains (54). Since PFO bound to and oligomerized on POPC membranes containing 48 mol% or more cholesterol (Figures 1A and 3), the total sterol concentration was fixed at 48 mol% of total lipids and POPC was used as the phospholipid in the following experiments. NBD-PFO was incubated with the various liposome preparations, and the extent of PFO binding and oligomerization was detected by visualization of SDS-resistant oligomeric bands. When the membrane was composed of only POPC and epicholesterol, no PFO oligomerization was detected (Figure 6, lane A). This result confirms previous data regarding PFO's inability to interact with a sterol having the OH group in the α-configuration (1,26). As the ratio of cholesterol/epicholesterol increased (Figure 6, lanes B–F), PFO oligomers began to form until the majority of PFO was present as an oligomeric species. Interestingly, when only 19 mol% cholesterol was present in the membrane, SDS-resistant PFO oligomers appeared (Figure 6, lane C). This result appears to conflict with our earlier findings that PFO required a minimum of 45 mol% cholesterol in POPC membranes to bind and form detectable oligomers. However, the membranes used in this sterol supplementation experiment contained a substantial amount of epicholesterol to maintain the total sterol concentration at 48 mol% in the membranes. Thus, while at least 45 mol% cholesterol was required for PFO binding when POPC/cholesterol liposomes were examined (Figure 1A), more than half of those sterol molecules were not directly involved in PFO–membrane interactions. The simplest explanation for this observation is that most of the sterol molecules in the bilayer are tightly packed with the phospholipids and hence not available to interact with PFO.

## DISCUSSION

Our examination of the cholesterol dependence of PFO binding to and interaction with membranes has provided insights into the mechanisms by which PFO accomplishes the initial cholesterol recognition step during pore formation. By applying a number of different experimental approaches, we were able to assess several different possibilities for the nature of the PFO–cholesterol interaction and ultimately identify the most important factor in determining whether PFO binds to the membrane surface. This factor, the presence of free cholesterol in the membrane, is critical for triggering the PFO–membrane interaction, while the packing of the acyl chains of the phospholipids and the nature of the phospholipids in the bilayer are only important to the extent that they influence cholesterol chemical activity or the exposure of cholesterol to the surface (55,56).

This conclusion is based primarily on the epicholesterol data that revealed that the efficacy of PFO binding to the membrane surface was dictated by both the presence of cholesterol and the total sterol content in the bilayer (Figure 6). PFO binds directly to pure cholesterol (26), but PFO–membrane recognition and binding requires PFO to access cholesterol that is membrane-embedded, yet surface-exposed. Cholesterol interacts more favorally with saturated acyl chain lipids than with unsaturated acyl chains lipids (ref 41 and references cited therein), and recent studies with monolayers and bilayers have demonstrated the existence of cholesterol-enriched regions in membranes whose formation is heavily dependent on the degree of phospholipid acyl chain unsaturation, head-group structure, and acyl chain length (56–59). Since epicholesterol has similar membrane packing characteristics as cholesterol (60), but is not

functional in PFO pore formation [Figure 6, lane A; (26)], the ability to partially replace cholesterol with epicholesterol without blocking PFO binding and oligomerization shows that some sterols in the membrane associate with phospholipids while others are free to interact directly with PFO. Hence, PFO binding was observed to membranes containing as little as 19 mol% cholesterol because the added epicholesterol (Figure 6, lane C) associates and interacts with phospholipids in the membrane allowing some of the cholesterol molecules to be free to interact with PFO. Epicholesterol apparently intercalates in the bilayer and competes with cholesterol for association with phospholipids, as reported for other membrane intercalating agents (61). These data therefore reveal that there are at least two distinctive states of cholesterol in a typical membrane bilayer: one in which cholesterol is readily accessible for binding to proteins such as PFO (free cholesterol), and one in which the sterol is associated with surrounding membrane components that reduce its exposure to the surface (e.g., phospholipid head-groups may obscure access to sterols associated with phospholipid acyl chains).

Consistent with our view, recent work done on two other cytolysins that bind cholesterol (streptolysin O and *Vibrio cholerae* toxin) indicated that reducing the size of the phospholipid headgroup caused an increase in cholesterol exposure and consequently an increase in the binding of the cytolysins (62). We have confirmed these observations by replacing some of the choline-containing POPC with ethanolamine-bearing POPE, a phospholipid with the same acyl chains but a smaller headgroup. The addition of POPE reduced the amount of cholesterol required for PFO binding (data not shown). In contrast, the presence of 10 mol% POPS in a POPC/POPS/cholesterol mixture did not affect the binding profile of PFO when cholesterol is varied from 34 to 55 mol%, either in the presence or absence of 2 mM $Ca^{2+}$ (data not shown).

Similarly, PFO binding requires less cholesterol when the liposomal phospholipids contain unsaturated rather than saturated acyl chains [Figure 1; (29,30)], presumably because acyl chain kinks introduced by the double bonds occupied more space within the bilayer and therefore pushed adjacent sterols out from under the headgroup where they were less accessible to PFO. We also observed that less cholesterol was required for PFO binding when the phospholipid acyl chain length increased up to 18 carbons (Figure 1). It have been shown that sterol/phospholipid interactions are affected by the hydrophobic mismatch between these two lipids because the hydrophobic "length" of cholesterol is equivalent to the length of a PC with 17 carbon saturated acyl chains (41). Phospholipid acyl chains with more than 17 carbons must bend to accommodate the shorter cholesterol molecule, and as a consequence the cholesterol molecules are pushed out from under the headgroup and become more exposed to PFO. Thus, the steric demands and interactions of lipid molecules in the bilayer will influence whether or not cholesterol is accessible to PFO. These findings agreed with those reported previously (34), though no clear conclusions evolved from their more limited investigation.

We also examined other membrane properties that did not correlate with the cholesterol dependence of PFO binding to the membrane. The relative acyl chain packing was one such property, as PFO was just as capable of binding to membranes displaying a low amount of lipid order (i.e., DOPC/cholesterol) as to membranes having a more restricted lipid motion (i.e., DPPC/cholesterol) (Figure 3). In addition, we also investigated whether PFO had a preference for binding to detergent-resistant or detergent-soluble membranes. Using cold TX-100 as an assay for membrane resistant to solubilization, we found the PFO bound both to DOPC/cholesterol liposomes that were completely soluble in TX-100 and to DPPC/cholesterol liposomes that were insoluble in TX-100 (Figure 4). These data indicate that the detergent solubility properties of a liposome comprised of cholesterol and a single phospholipid does not correlate with the binding of PFO to the membrane.

However, when we examined more complex lipid mixtures containing DOPC, SM, and a constant amount of cholesterol, we discovered that the ratio of DOPC/SM in the membranes affected PFO binding and oligomerization (Figure 5). Increasing the SM content of the membranes enhanced their resistant to cold TX-100 solubilization and reduced the ability of PFO to recognize and/or bind to cholesterol. PFO binding to membranes therefore appeared to be negatively influenced by the presence of SM. More importantly, this result suggests that PFO does not recognize or bind to cholesterol that is sequestered in SM-rich microdomains, structures that are commonly associated with the presence of "rafts" in cell membranes (63).

Our data therefore conflict with an earlier report that PFO interacts preferentially with cholesterol located in lipid "rafts" in natural membranes (64,65). Their conclusions were based on the colocalization of a protease-treated PFO fragment with lipid raft-associated proteins during TX-100 detergent-insolubility assays. In our experience, such an experimental approach is susceptible to multiple interpretations and this may explain the difference between their conclusions and ours. Using the detergent and pelleting conditions reported in their work to examine PFO localization in "rafts", we found that the majority of the PFO was located in the pellet after treatment with TX-100 when either DOPC- or DPPC-liposomes containing 50 mol % cholesterol were used (data not shown). Since DOPC/cholesterol membranes were soluble in TX-100 (Figure 4), the PFO in the pellet was not bound to any detergent-resistant membranes. This result demonstrated that the membrane-inserted PFO oligomer was resistant to dissociation by either SDS or TX-100 since oligomeric PFO was found in the pellet. The resistance of the PFO oligomer to TX-100 solubilization may therefore complicate the interpretation of the sedimentation data because PFO oligomers may sediment in the presence of TX-100 even if they were formed on nonraft membrane surfaces. Since our data were obtained with full-length PFO and uniform chemically defined liposomes, we believe that PFO does not necessarily bind to lipid "rafts" in membranes. But we also recognize that the conflicting conclusions may reflect limitations in the TX-100 assay as applied to natural and/or synthetic membranes (47,50).

It is clear from the data presented in this work that the total amount of cholesterol required to trigger PFO binding to a particular membrane is influenced by the lipid composition of the bilayer. Moreover, the total amount of cholesterol required to initiate PFO binding will also be affected by the presence of membrane proteins due to specific lipid binding to, association with, or intercalation into the transmembrane segments of these proteins. We speculate that the latter effect may be the reason that PFO binds to and forms pores in ER membranes (37–39) even though their total cholesterol content is very low, because the nonsterol lipid components are more likely to pack within the membrane proteins than are the relatively rigid cholesterol molecules. One effect of this selective partitioning is that the mole fraction of cholesterol in the bulk lipid in the exposed membrane surface area will increase (35). Whatever the explanation for the sensitivity of ER membranes to PFO, one should be cautious when using PFO or any PFO derivatives to track the total cholesterol content in cellular membranes. PFO binding may depend on the "free cholesterol" or cholesterol chemical activity, rather than on the total amount of cholesterol present in the membrane, and the chemical activity will be influenced by the lipid composition and the presence of other membrane components.

In summary, exposure of free cholesterol at the membrane surface is essential for PFO binding to the bilayer and the initiation of the sequence of events that culminate with the spontaneous formation of a transmembrane pore. Bending of the phospholipids acyl chains by introducing double bonds or reducing the size of the phospholipid head groups decreased the threshold of cholesterol required to trigger binding. In contrast, changes in the relative packing of lipids in the membrane core or the presence or absence of detergent-resistant membranes did not correlate with PFO binding. Finally, addition of molecules that do not interact with PFO, but intercalate into the membrane and displace cholesterol from its association with phospholipids

(e.g., epicholesterol), reduced the amount of cholesterol required to trigger PFO binding. Since exposure of free cholesterol at the surface of membranes is necessary for the binding of CDCs and other bacterial and viral proteins (15,66–70), the results reported here may be generally applicable to other protein–membrane interactions involved in human pathogenesis.

## Supplementary Material

Refer to Web version on PubMed Central for supplementary material.

## Acknowledgments

We thank Dr. Paul Moe for critically reading the manuscript.

## References

1. Alouf, JE.; Billington, SJ.; Jost, BH. Repertoire and general features of the family of cholesterol-dependent cytolysins. In: Alouf, JE.; Popoff, MR., editors. The Comprehensive Sourcebook of Bacterial Protein Toxins. Academic Press; Oxford, England: 2005. p. 643-658.
2. Mosser E, Rest R. The *Bacillus anthracis* cholesterol-dependent cytolysin, anthrolysin O, kills human neutrophils, monocytes and macrophages. BMC Microbiol 2006;6:56. [PubMed: 16790055]
3. Farrand S, Hotze E, Friese P, Hollingshead SK, Smith DF, Cummings RD, Dale GL, Tweten RK. Characterization of a streptococcal cholesterol-dependent cytolysin with a lewis y and b specific lectin domain. Biochemistry 2008;47:7097–7107. [PubMed: 18553932]
4. Gelber SE, Aguilar JL, Lewis KLT, Ratner AJ. Functional and phylogenetic characterization of vaginolysin, the human-specific cytolysin from *Gardnerella vaginalis*. J Bacteriol 2008;190:3896–3903. [PubMed: 18390664]
5. Polekhina G, Giddings KS, Tweten RK, Parker MW. Insights into the action of the superfamily of cholesterol-dependent cytolysins from studies of intermedilysin. Proc Natl Acad Sci U S A 2005;102:600–605. [PubMed: 15637162]
6. Tweten RK. Cholesterol-dependent cytolysins, a family of versatile pore-forming toxins. Infect Immun 2005;73:6199–6209. [PubMed: 16177291]
7. Rosado CJ, Buckle AM, Law RHP, Butcher RE, Kan WT, Bird CH, Ung K, Browne KA, Baran K, Bashtannyk-Puhalovich TA, Faux NG, Wong W, Porter CJ, Pike RN, Ellisdon AM, Pearce MC, Bottomley SP, Emsley J, Smith AI, Rossjohn J, Hartland EL, Voskoboinik I, Trapani JA, Bird PI, Dunstone MA, Whisstock JC. A common fold mediates vertebrate defense and bacterial attack. Science 2007;317:1548–1551. [PubMed: 17717151]
8. Hadders MA, Beringer DX, Gros P. Structure of C8α-MACPF reveals mechanism of membrane attack in complement immune defense. Science 2007;317:1552–1554. [PubMed: 17872444]
9. Giddings, KS.; Johnson, AE.; Tweten, RK. Perfringolysin O and intermedilysin: Mechanisms of pore formation by the cholesterol-dependent cytolysins. In: Alouf, JE.; Popoff, MR., editors. The Comprehensive Sourcebook of Bacterial Protein Toxins. Academic Press; Oxford, England: 2005. p. 671-679.
10. Olofsson A, Hebert H, Thelestam M. The projection structure of perfringolysin O (*Clostridium perfringens* -toxin). FEBS Lett 1993;319:125–127. [PubMed: 8454043]
11. Czajkowsky DM, Hotze EM, Shao Z, Tweten RK. Vertical collapse ofa cytolysin prepore moves its transmembrane beta-hairpins to the membrane. EMBO J 2004;23:3206–3215. [PubMed: 15297878]
12. Dang TX, Hotze EM, Rouiller I, Tweten RK, Wilson-Kubalek EM. Prepore to pore transition of a cholesterol-dependent cytolysin visualized by electron microscopy. J Struct Biol 2005;150:100–108. [PubMed: 15797734]
13. Tilley SJ, Orlova EV, Gilbert RJ, Andrew PW, Saibil HR. Structural basis of pore formation by the bacterial toxin pneumolysin. Cell 2005;121:247–256. [PubMed: 15851031]
14. Palmer M. Cholesterol and the activity of bacterial toxins. FEMS Microbiol Lett 2004;238:281–289. [PubMed: 15358412]

15. Umashankar M, Sanchez San Martin C, Liao M, Reilly B, Guo A, Taylor G, Kielian M. Differential cholesterol binding by class II fusion proteins determines membrane fusion properties. J Virol 2008;82:9245–9253. [PubMed: 18632857]
16. Giddings KS, Zhao J, Sims PJ, Tweten RK. Human CD59 is a receptor for the cholesterol-dependent cytolysin intermedilysin. Nat Struct Mol Biol 2004;11:1173–1178. [PubMed: 15543155]
17. Giddings KS, Johnson AE, Tweten RK. Redefining cholesterol's role in the mechanism of the cholesterol-dependent cytolysins. Proc Natl Acad Sci U S A 2003;100:11315–11320. [PubMed: 14500900]
18. Heuck AP, Tweten RK, Johnson AE. Beta-barrel pore-forming toxins: Intriguing dimorphic proteins. Biochemistry 2001;40:9065–9073. [PubMed: 11478872]
19. Heuck AP, Hotze EM, Tweten RK, Johnson AE. Mechanism of membrane insertion of a multimeric -barrel protein: Perfringolysin O creates a pore using ordered and coupled conformational changes. Mol Cell 2000;6:1233–1242. [PubMed: 11106760]
20. Rossjohn J, Feil SC, McKinstry WJ, Tweten RK, Parker MW. Structure of a cholesterol-binding, thiol-activated cytolysin and a model of its membrane form. Cell 1997;89:685–692. [PubMed: 9182756]
21. Ramachandran R, Heuck AP, Tweten RK, Johnson AE. Structural insights into the membrane-anchoring mechanism of a cholesterol-dependent cytolysin. Nat Struct Mol Biol 2002;9:823–82.
22. Soltani CE, Hotze EM, Johnson AE, Tweten RK. Specific protein-membrane contacts are required for prepore and pore assembly by a cholesterol-dependent cytolysin. J Biol Chem 2007;282:15709–15716. [PubMed: 17412689]
23. Ramachandran R, Tweten RK, Johnson AE. Membrane-dependent conformational changes initiate cholesterol-dependent cytolysin oligomerization and intersubunit beta-strand alignment. Nat Struct Mol Biol 2004;11:697–705. [PubMed: 15235590]
24. Soltani CE, Hotze EM, Johnson AE, Tweten RK. Structural elements of the cholesterol-dependent cytolysins that are responsible for their cholesterol-sensitive membrane interactions. Proc Natl Acad Sci U S A 2007;104:20226–20231. [PubMed: 18077338]
25. Rossjohn J, Polekhina G, Feil SC, Morton CJ, Tweten RK, Parker MW. Structures of perfringolysin O suggest a pathway for activation of cholesterol-dependent cytolysins. J Mol Biol 2007;367:1227–1236. [PubMed: 17328912]
26. Heuck AP, Savva CG, Holzenburg A, Johnson AE. Conformational changes that effect oligomerization and initiate pore formation are triggered throughout perfringolysin O upon binding to cholesterol. J Biol Chem 2007;282:22629–22637. [PubMed: 17553799]
27. Heuck, AP.; Johnson, AE. Membrane recognition and pore formation by bacterial pore-forming toxins. In: Tamm, LK., editor. Protein–Lipid Interactions from Membrane Domains to Cellular Networks. Wiley-VCH; Weinheim: 2005. p. 163-186.
28. Ohno-Iwashita Y, Shimada Y, Waheed A, Hayashi M, Inomata M, Nakamura M, Maruya M, Iwashita M. Perfringolysin O, a cholesterol-binding cytolysin, as a probe for lipid rafts. Anaerobe 2004:125–134. [PubMed: 16701509]
29. Nelson LD, Johnson AE, London E. How interaction of perfringolysin O with membranes is controlled by sterol structure, lipid structure, and physiological low pH: Insights into the origin of perfringolysin o-lipid raft interaction. J Biol Chem 2008;283:4632–4642. [PubMed: 18089559]
30. Flanagan JJ, Heuck AP, Johnson AE. Cholesterol-phospholipid interactions play an important role in perfringolysin O binding to membrane. FASEB J 2002;16:A929.
31. Shepard LA, Heuck AP, Hamman BD, Rossjohn J, Parker MW, Ryan KR, Johnson AE, Tweten RK. Identification of a membrane-spanning domain of the thiol-activated pore-forming toxin *Clostridium perfringens* perfringolysin O: An α-helical to -sheet transition identified by fluorescence spectroscopy. Biochemistry 1998;37:14563–14574. [PubMed: 9772185]
32. Heuck AP, Tweten RK, Johnson AE. Assembly and topography of the prepore complex in cholesterol-dependent cytolysins. J Biol Chem 2003;278:31218–31225. [PubMed: 12777381]
33. Shepard LA, Shatursky O, Johnson AE, Tweten RK. The mechanism of pore assembly for a cholesterol-dependent cytolysin: Formation of a large prepore complex precedes the insertion of the transmembrane beta-hairpins. Biochemistry 2000;39:10284–10293. [PubMed: 10956018]

34. Ohno-Iwashita Y, Iwamoto M, Ando S, Iwashita S. Effect of lipidic factors on membrane cholesterol topology - mode of binding of -toxin to cholesterol in liposomes. Biochim Biophys Acta 1992;1109:81–90. [PubMed: 1504083]
35. Lange Y, Steck TL. Cholesterol homeostasis and the escape tendency (activity) of plasma membrane cholesterol. Prog Lipid Res 2008;47:319–332. [PubMed: 18423408]
36. van Meer G, Voelker DR, Feigenson GW. Membrane lipids: Where they are and how they behave. Nat Rev Mol Cell Biol 2008;9:112–124. [PubMed: 18216768]
37. Crowley KS, Liao S, Worrell VE, Reinhart GD, Johnson AE. Secretory proteins move through the endoplasmic reticulum membrane via an aqueous, gated pore. Cell 1994;78:461–471. [PubMed: 8062388]
38. Hamman BD, Hendershot LM, Johnson AE. BiP maintains the permeability barrier of the ER membrane by sealing the lumenal end of the translocon pore before and early in translocation. Cell 1998;92:747–758. [PubMed: 9529251]
39. Alder NN, Shen Y, Brodsky JL, Hendershot LM, Johnson AE. The molecular mechanisms underlying BiP-mediated gating of the Sec61 translocon of the endoplasmic reticulum. J Cell Biol 2005;168:389–399. [PubMed: 15684029]
40. Shatursky O, Heuck AP, Shepard LA, Rossjohn J, Parker MW, Johnson AE, Tweten RK. The mechanism of membrane insertion for a cholesterol-dependent cytolysin: A novel paradigm for pore-forming toxins. Cell 1999;99:293–299. [PubMed: 10555145]
41. Ohvo-Rekilä H, Ramstedt B, Leppimäki P, Peter Slotte J. Cholesterol interactions with phospholipids in membranes. Prog Lipid Res 2002;41:66–97. [PubMed: 11694269]
42. Halling KK, Ramstedt B, Nystrom JH, Slotte JP, Nyholm TKM. Cholesterol interactions with fluid phase phospholipids: Effect on the lateral organization of the bilayer. Biophys J 2008;95:3861–3871. [PubMed: 18641061]
43. Andrich MP, Vanderkooi JM. Temperature dependence of 1,6-diphenyl-1,3,5-hexatriene fluorescence in phospholipid artificial membranes. Biochemistry 1976;15:1257–1261. [PubMed: 1252446]
44. Schroeder RJ, Ahmed SN, Zhu Y, London E, Brown DA. Cholesterol and sphingolipid enhance the Triton X-100 insolubility of glycosylphosphatidylinositol-anchored proteins by promoting the formation of detergent-insoluble ordered membrane domains. J Biol Chem 1998;273:1150–1157. [PubMed: 9422781]
45. Sankaram MB, Thompson TE. Cholesterol-induced fluid-phase immiscibility in membranes. Proc Natl Acad Sci U S A 1991;88:8686–8690. [PubMed: 1656453]
46. de Almeida RF, Fedorov A, Prieto M. Sphingomyelin/phosphatidylcholine/cholesterol phase diagram: Boundaries and composition of lipid rafts. Biophys J 2003;85:2406–2416. [PubMed: 14507704]
47. Lichtenberg D, Goni FM, Heerklotz H. Detergent-resistant membranes should not be identified with membrane rafts. Trends Biochem Sci 2005;30:430–436. [PubMed: 15996869]
48. Reyes Mateo C, Ulises Acuna A, Brochon JC. Liquid-crystalline phases of cholesterol/lipid bilayers as revealed by the fluorescence of trans-parinaric acid. Biophys J 1995;68:978–987. [PubMed: 7756560]
49. Solovyova AS, Nollmann M, Mitchell TJ, Byron O. The solution structure and oligomerization behavior of two bacterial toxins: Pneumolysin and perfringolysin O. Biophys J 2004;87:540–552. [PubMed: 15240487]
50. London E, Brown DA. Insolubility of lipids in Triton X-100: Physical origin and relationship to sphingolipid/cholesterol membrane domains (rafts). Biochim Biophys Acta 2000;1508:182–195. [PubMed: 11090825]
51. Hase J, Mitsui K, Shonaka E. *Clostridium perfringens* exotoxins. IV. Inhibition of the theta-toxin induced hemolysis by steroids and related compounds. Jpn J Exp Med 1976;46:45–50. [PubMed: 180313]
52. Prigent D, Alouf JE. Interaction of streptolysin O with sterols. Biochim Biophys Acta 1976;443:288–300. [PubMed: 182263]
53. Alouf JE, Geoffroy C, Pattus F, Verger R. Surface properties of bacterial sulfhydryl-activated cytolytic toxins. Eur J Biochem 1984;141:205–210. [PubMed: 6723658]

54. Samsonov AV, Mihalyov I, Cohen FS. Characterization of cholesterol-sphingomyelin domains and their dynamics in bilayer membranes. Biophys J 2001;81:1486–1500. [PubMed: 11509362]
55. Huang J, Feigenson GW. A microscopic interaction model of maximum solubility of cholesterol in lipid bilayers. Biophys J 1999;76:2142–2157. [PubMed: 10096908]
56. Radhakrishnan A, McConnell HM. Chemical activity of cholesterol in membranes. Biochemistry 2000;39:8119–8124. [PubMed: 10889017]
57. Crane JM, Tamm LK. Role of cholesterol in the formation and nature of lipid rafts in planar and spherical model membranes. Biophys J 2004;86:2965–2979. [PubMed: 15111412]
58. Silvius JR. Role of cholesterol in lipid raft formation: Lessons from lipid model systems. Biochim Biophys Acta 2003;1610:174–183. [PubMed: 12648772]
59. Veatch SL, Keller SL. Miscibility phase diagrams of giant vesicles containing sphingomyelin. Phys Rev Lett 2005;94:148101–148104. [PubMed: 15904115]
60. Beattie ME, Veatch SL, Stottrup BL, Keller SL. Sterol structure determines miscibility versus melting transitions in lipid vesicles. Biophys J 2005;89:1760–1768. [PubMed: 15951379]
61. Lange Y, Ye J, Steck TL. Activation of membrane cholesterol by displacement from phospholipids. J Biol Chem 2005;280:36126–36131. [PubMed: 16129675]
62. Zitzer A, Westover EJ, Covey DF, Palmer M. Differential interaction of the two cholesterol-dependent, membrane-damaging toxins, streptolysin O and *Vibrio cholerae* cytolysin, with enantiomeric cholesterol. FEBS Lett 2003;553:229–231. [PubMed: 14572629]
63. Pike LJ. Rafts defined: A report on the Keystone symposium on lipid rafts and cell function. J Lipid Res 2006;47:1597–1598. [PubMed: 16645198]
64. Shimada Y, Maruya M, Iwashita S, Ohno-Iwashita Y. The C-terminal domain of perfringolysin O is an essential cholesterol-binding unit targeting to cholesterol-rich microdomains. Eur J Biochem 2002;269:6195–6203. [PubMed: 12473115]
65. Waheed A, Shimada Y, Heijnen HFG, Nakamura M, Inomata M, Hayashi M, Iwashita S, Slot JW, Ohno-Iwashita Y. Selective binding of perfringolysin O derivative to cholesterol-rich membrane microdomains (rafts). Proc Natl Acad Sci U S A 2001;98:4926–4931. [PubMed: 11309501]
66. Alving CR, Habig WH, Urban KA, Hardegree MC. Cholesterol-dependent tetanolysin damage to liposomes. Biochim Biophys Acta 1979;551:224–228. [PubMed: 427152]
67. Rosenqvist E, Michaelsen TE, Vistnes AI. Effect of streptolysin O and digitonin on egg Lecithin/cholesterol vesicles. Biochim Biophys Acta 1980;600:91–102. [PubMed: 6249363]
68. Barlic A, Gutierrez-Aguirre I, Caaveiro JM, Cruz A, Ruiz-Arguello MB, Perez-Gil J, Gonzalez-Manas JM. Lipid phase coexistence favors membrane insertion of equinatoxin-II, a pore-forming toxin from *Actinia equina*. J Biol Chem 2004;279:34209–34216. [PubMed: 15175339]
69. Chattopadhyay K, Bhattacharyya D, Banerjee KK. *Vibrio cholerae* hemolysin. Eur J Biochem 2002;269:4351–4358. [PubMed: 12199714]
70. Giesemann T, Jank T, Gerhard R, Maier E, Just I, Benz R, Aktories K. Cholesterol-dependent pore formation of *Clostridium difficile* toxin A. J Biol Chem 2006;281:10808–10815. [PubMed: 16513641]

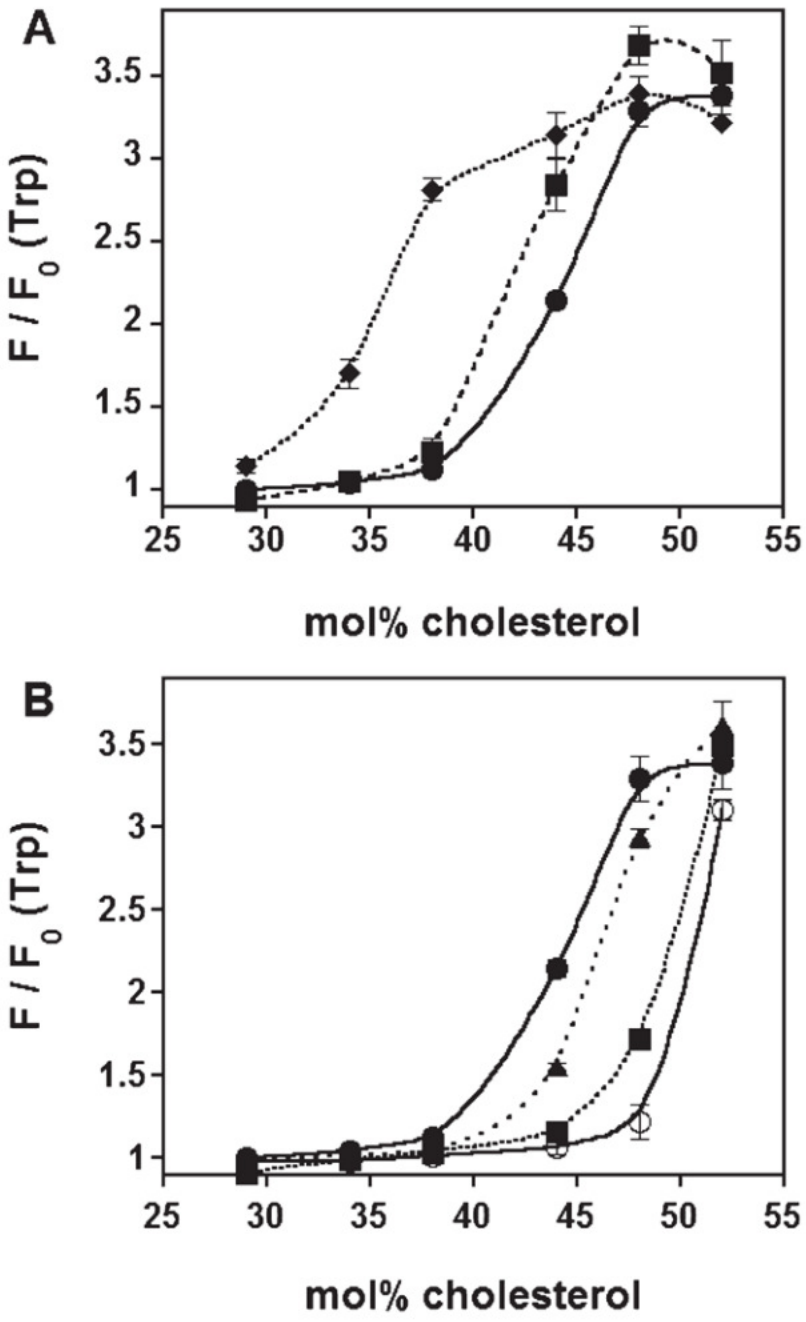


**Figure 1.**

Cholesterol dependence of PFO binding to liposomes composed of cholesterol and various phospholipids. Changes in the PFO Trp emission intensity are shown as a function of the cholesterol content of the different liposomes. The net $F/F_0$ was calculated as described in Experimental Procedures. (A) DOPC, ◆ ; SOPC, ■; POPC, ●. (B) DSPC, ▲; DPPC, ■; DMPC, ○. The cholesterol dependence curve for POPC (●) is shown for reference. Error bars indicate the standard deviation observed for three independent measurements per data point.

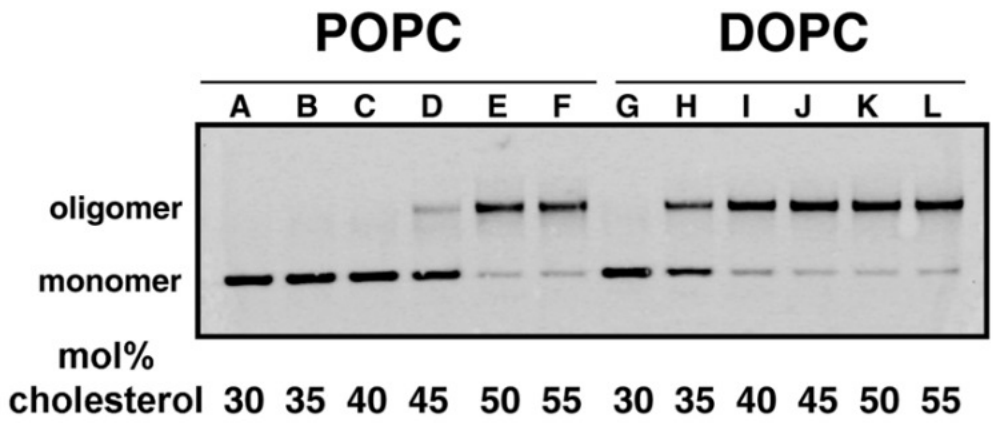


**Figure 2.**

Cholesterol dependence of PFO oligomerization on POPC- or DOPC-cholesterol liposomes. The amount of cholesterol present in the PC-liposomes is shown below each lane. Lanes A–F show PFO oligomerization with POPC/cholesterol liposomes, while lanes G–L contain DOPC/cholesterol liposomes. The NBD-PFO monomer and oligomer bands were visualized with a BioRad Molecular Imager FX as described in the Experimental Procedures.

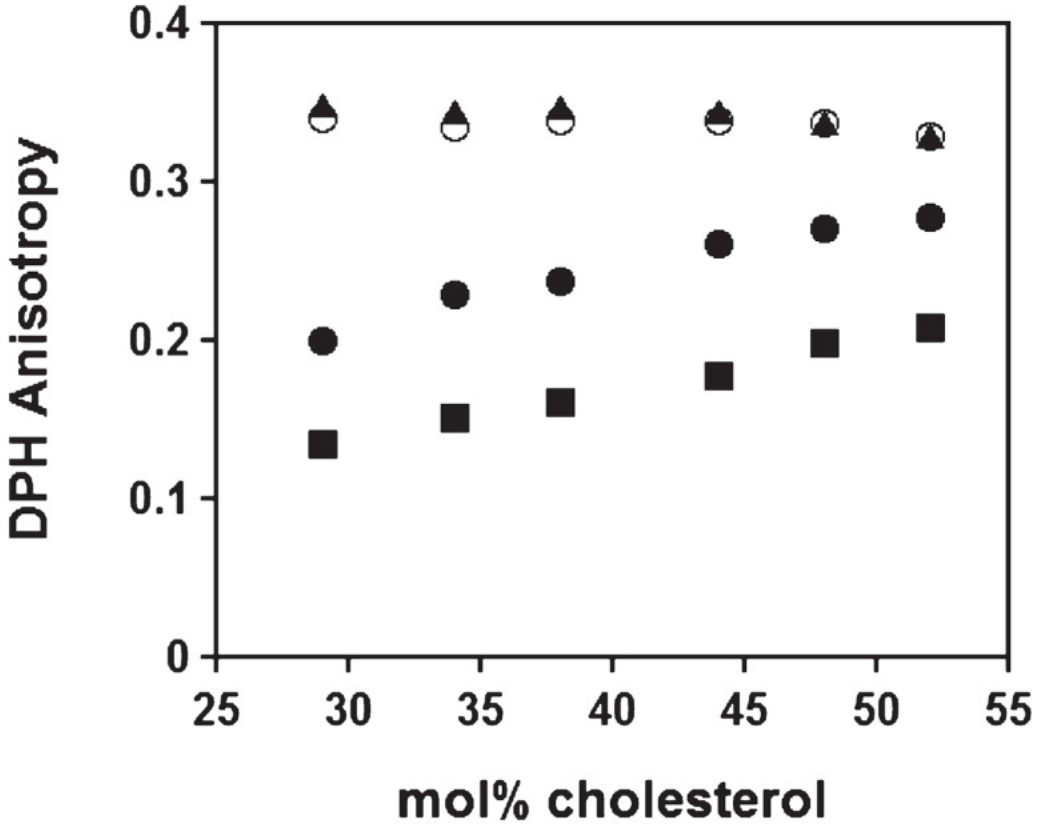


**Figure 3.**
Effect of cholesterol concentration and phospholipid unsaturation on lipid order in liposomes as measured by DPH anisotropy. DPH was incorporated into the PC/cholesterol membranes as described in Experimental Procedures. DPPC, ▲; DSPC, ○; POPC, ●; DOPC, ■.

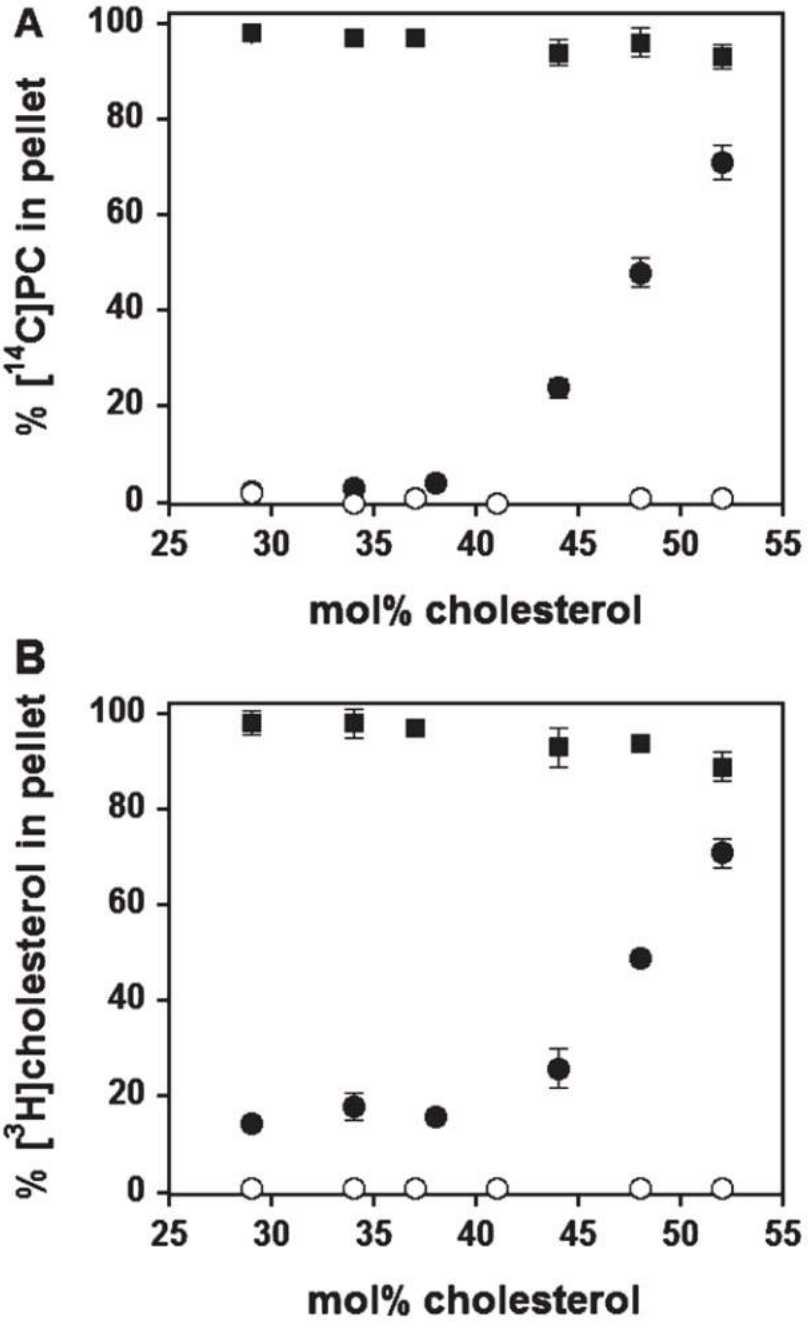


**Figure 4.**

Detergent insolubility of various PC/cholesterol liposomes. Liposomes with trace amounts of [$^3$H]cholesterol and [$^{14}$C] PC were extracted with TX-100 at 0 °C. Radioactivity in the pellet fractions was measured after ultracentrifugation, and the percent of radioactivity in the pellet was plotted as a function of cholesterol concentration. (A) Fraction of [$^3$H]cholesterol found in pellet. (B) Fraction of [$^{14}$C]PC found in pellet. In both (A) and (B), the PC species are the following: DOPC, ○; POPC, ●; and DPPC, ■.

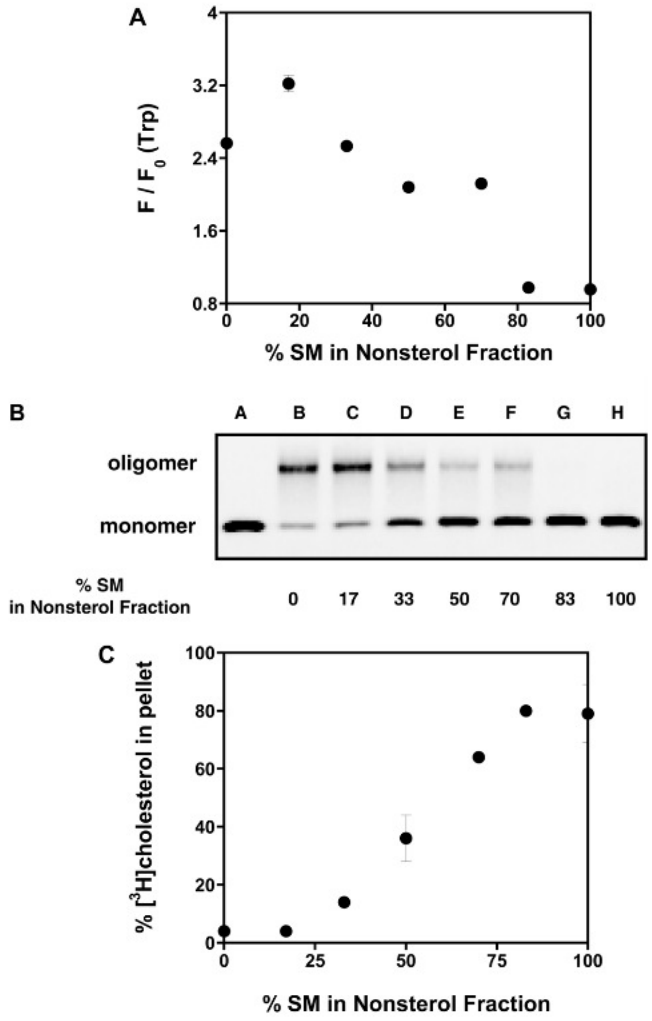


**Figure 5.**

PFO binding to DOPC/SM/cholesterol membranes. (A) Changes in the Trp emission intensity of PFO are shown as a function of the percentage of SM in the nonsterol fraction of the membranes. The net $F/F_0$ was calculated as described in Experimental Procedures. Error bars indicate the standard deviation observed for three independent measurements per data point. (B) NBD-PFO oligomerization on DOPC/SM/cholesterol membranes. After incubation of PFO with the membranes, samples were solubilized with sample buffer and separated by 1.5% SDS–AGE. The NBD-PFO monomer and oligomer bands were visualized with a BioRad Molecular Imager FX as described in the Experimental Procedures. In both (A) and (B), the membranes were composed of 50 mol% cholesterol and various proportions of DOPC and SM comprising the remaining 50 mol% lipid in the nonsterol fraction. For example, when SM is at 50% in the nonsterol fraction, there is an equimolar amount of SM and DOPC (25 mol% each). (C). Formation of detergent-resistant domains in DOPC/SM/cholesterol membranes. The liposomes were composed of 40 mol% cholesterol and various proportions of DOPC and SM comprising the remaining 60 mol% lipid in the nonsterol fraction. Liposomes with trace amounts of [$^3$H] cholesterol were extracted with TX-100 at 0 °C. Radioactivity in the pellet fractions was measured after ultracentrifugation, and the percent of radioactivity in the pellet was plotted as a function of the percentage of SM in the nonsterol fraction of the membrane.

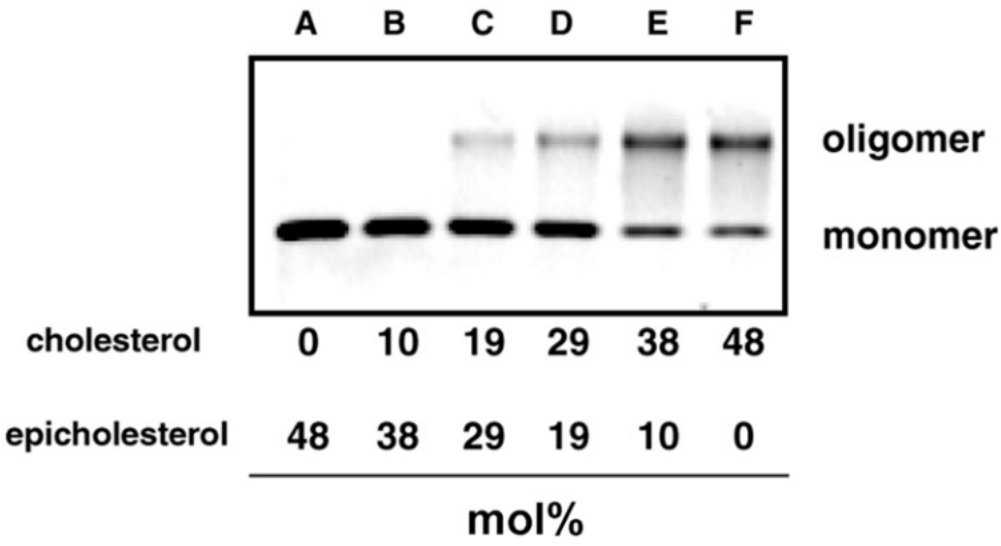


**Figure 6.**

NBD-PFO oligomerization on membranes containing cholesterol and epicholesterol. The liposomes contained 52 mol% POPC and 48 mol% sterol. The mol% of the individual sterols comprising the sterol fraction of the liposome is indicated below each lane in the above figure. After incubation of PFO with the membranes, samples were solubilized with sample buffer and separated by 1.5% SDS–AGE. The NBD-PFO monomer and oligomer bands were visualized with a BioRad Molecular Imager FX as described in the Experimental Procedures.

**Table 1**

Names and Acyl-Chain Properties of PCs Used to Prepare Liposomes

| abbreviation | 1-acyl | carbons: double bonds | 2-acyl | carbons: double bonds |
|---|---|---|---|---|
| POPC | palmitoyl | 16:0 | oleoyl | 18:1 (Δ9) |
| DOPC | oleoyl | 18:1 (Δ9) | oleoyl | 18:1 (Δ9) |
| SOPC | stearoyl | 18:0 | oleoyl | 18:1 (Δ9) |
| DMPC | myristoyl | 14:0 | myristoyl | 14:0 |
| DPPC | palmitoyl | 16:0 | palmitoyl | 16:0 |
| DSPC | stearoyl | 18:0 | stearoyl | 18:0 |